ORGANOMETALLICS

Article

pubs.acs.org/Organometallics

Synthesis, Solid-State Structures, and Computational Studies of Half-Sandwich Cp*BeX (X = Cl, Br, I) Compounds

Dominik Naglav, Briac Tobey, Anja Neumann, Dieter Bläser, Christoph Wölper, and Stephan Schulz*

Institute of Inorganic Chemistry, University of Duisburg-Essen, 45117 Essen, Germany

Supporting Information

ABSTRACT: The solid-state structures of half-sandwich beryllium complexes Cp*BeX (X = Cl (**1**), Br (**2**), I (**3**)) are described. All attempts to synthesize Cp*BeF (**4**) by reaction of **1**−**3** with several fluorinating reagents such as AgF_2, XeF_2, 4-$FC_6H_4IF_2$, AgF, NaF, and Me_4NF failed. However, the reaction of **3** and AgF in resulted in the unexpected synthesis of the known beryllocene $Cp*_2Be$ (**5**). Quantum-chemical calculations were performed to investigate the electronic structures of **1**−**4**.

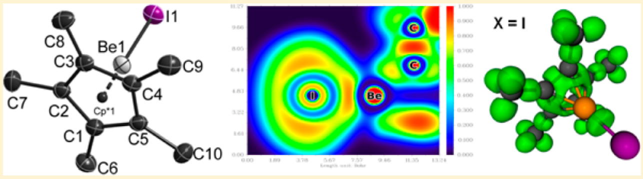

INTRODUCTION

Metallocenes of group 2 metals of the type MCp_2 (Cp = C_5H_5) as well as those containing sterically more bulky cyclopentadienyl ligands such as Cp′ (C_5Me_4H) and Cp* (C_5Me_5) have been investigated in detail in recent years.[1] The most prominent difference within this class of compounds is reflected by the different bonding situations. While metallocenes containing the heavier group 2 metals show predominantly ionic bonding contributions, which amount to approximately 70−85% of the total interaction energy,[1a,2] the corresponding beryllium complexes exhibit higher covalent bonding character. Moreover, the number of structurally characterized beryllocenes is much smaller compared with their heavier congeners.[3] To the best of our knowledge, only Cp_2Be,[4,5,6d] $Cp*_2Be$,[6a,c,d] Cp'_2Be,[6c,d] and Cp*BeCp′[6b,c] have been structurally characterized by single-crystal X-ray analysis to date. Cp_2Be adopts a slip-sandwich η^5/η^1 structure in which the Be atom is disordered between two crystallographically equivalent sites of 50% occupancy. The different nature of the two Cp rings is preserved in solution, as indicated by the high dipole moment, for which different values have been reported[4] (i.e., 2.24 D in cyclohexane, 2.46 D in benzene at 25 °C[4a]), as well as in the gas phase, as shown by gas-phase electron diffraction[7] and quantum-chemical calculations.[8] However, NMR spectroscopic studies proved that Cp_2Be undergoes fast rearrangement reactions in solution,[9] which according to theoretical calculations[10] occur through two dynamic processes, namely a 1,5 sigmatropic shift of the η^5-CpBe unit around the periphery of the η^1-Cp ring (activation energy 5 kJ mol^{-1}; η^5/η^2 transition state) and a molecular inversion mechanism that interchanges the η^5-Cp and η^1-Cp rings (activation energy 8 kJ mol^{-1}; η^3/η^3 transition state). The activation energy for the molecular inversion of Cp_2Be in the solid state was experimentally determined by Hung et al. to 36.9 kJ mol^{-1}.[6d] Comparable slip-sandwich structures in the solid state were reported for Cp'_2Be[6c,d] and Cp*BeCp′,[6b,c] whereas $Cp*_2Be$[6a,c,d] adopts a regular sandwich structure with two η^5-bonded Cp* groups. Even more surprisingly, the solid-state structures of the corresponding half-sandwich complexes Cp*BeX (X = halide) are unknown,[11] while heteroleptic CpBeX complexes such as CpBeCl and $CpBeSiMe_3$ have been structurally characterized.[12] Very recently, Krossing and co-workers reported the synthesis and structure of Cp*Be−F−$Al(OR^F)_3$ upon reaction of Cp*BeBr with $Ag[Al(OR^F)_4]$. During this reaction, one of the 36 equivalent C−F bonds of the $[Al(OR_F)_4]^-$ anion was activated by the highly electrophilic $[Cp*Be]^+$ cation, resulting in the formation of a $[F-Al(OR^F)_3]^-$ anion.[13]

We recently became interested in the synthesis of homo- and heteroleptic Be complexes and reported the structures of several 1-tris(pyrazolyl)borate beryllium halides TpBeX as well as the solid-state structure of $Be[N(SiMe_3)_2]_2$.[14] Herein we report the synthesis and solid-state structures of heteroleptic, donor-free pentamethylcyclopentadienyl beryllium halides Cp*BeX (X = Cl (**1**), Br (**2**), I (**3**)) as well as of $Cp*_2Be$. In addition, their structures were investigated by quantum-chemical calculations, and results from natural bond orbital, electron localization function, and localized orbital locator analyses are presented.

RESULTS AND DISCUSSION

Synthesis of 1−3. Cp*BeCl can be prepared by the reaction of $BeCl_2(OEt_2)_2$ with either $Cp*_2Mg$[15] or Cp*Li,[16] and Cp*BeBr can be obtained by the reaction of Cp*Na with $BeBr_2$.[11] We synthesized Cp*BeX **1**−**3** using a slightly modified procedure by the reaction of BeX_2 (X = Cl, Br, I) and Cp*K (Scheme 1). The two compounds were mixed as solids and suspended in dry toluene. The reaction mixture was then stirred for at least 16 h at ambient temperature to give **1**−**3** in good yields (>50%). Toluene was used as the solvent since both starting reagents are insoluble in this solvent but the

Received: May 7, 2015

DOI: 10.1021/acs.organomet.5b00389
Organometallics XXXX, XXX, XXX−XXX

Scheme 1. Synthesis of 1 to 3

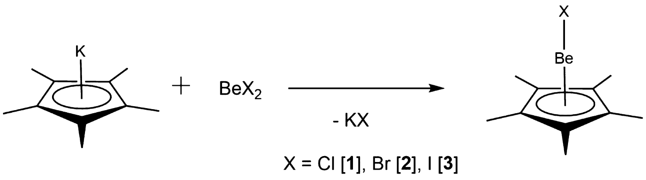

product dissolves very well. A coordinating solvent such as tetrahydrofuran (THF) or Et_2O can also be used, as **1**−**3** do not show any sign of formation of the corresponding solvent-stabilized compounds. The yields can be substantially improved by stirring the reaction mixture for 3 days at room temperature or for 12 h at 60 °C. Pure **1**−**3** were isolated in very high yields (**1**, 86%; **2**, 85%; **3**, 92%) as large, colorless blocklike crystals after filtration of any insoluble material and storage of the resulting concentrated solutions at 6 °C. **1**−**3** are extremely sensitive toward oxygen or water and also decompose rapidly in the presence of impurities such as grease. Therefore, the synthesis of **1**−**3** is best performed in closed apparatuses with Young-type stopcocks, such as a double Schlenk flask equipped with a glass frit.

The ^{1}H and ^{13}C NMR spectra of **1**−**3** show the expected resonances of the Cp* ligand. The ^{1}H NMR spectra of **1**−**3** show a single resonance for the magnetically equivalent Me groups (1.68 pm for **1**, 1.67 pm for **2**, and 1.65 pm for **3** in C_6D_6, compared with 1.81 ppm for $Cp^*{}_2Be$,[6c] 1.67 ppm for Cp*BeCl,[15] 1.66 ppm for Cp*BeBr,[11] 1.76 ppm for Cp*BeMe,[17] and 1.59 ppm for Cp*BeCp′[6c]). The ^{13}C NMR spectra of **1**−**3** each show a single resonance for the ring carbon atoms (109.95 pm for **1**, 110.21 pm for **2**, and 110.53 pm for **3** in C_6D_6), indicating η^5-bonded Cp* groups. Comparable findings were reported for homo- and heteroleptic η^5-Cp*BeX compounds such as $Cp^*{}_2Be$ (110.4 ppm),[6c] Cp*BeCp (108.6 ppm),[16] Cp*BeCl (109.6 ppm),[16] Cp*BeMe (108.0 ppm),[17] Cp*BeCp′ (108.9 ppm),[6c] Cp*BeCNXylCp* (108.8 ppm),[18] and $Cp^*BeP(t\text{-}Bu)_2$[19] and $Cp^*BeAs(t\text{-}Bu)_2$ (109.3 ppm).[20] In addition, $^{9}Be\{^{1}H\}$ NMR spectra (Table 1) gave resonances at −14.9 ppm for **1**, −14.8 ppm for **2**, and −15.8 ppm for **3**, which compare well with values reported for $Cp^*{}_2Be$ (−21.7 ppm, $w_{1/2}$ = 4.4 Hz)[6c,15] and Cp*BeCp′ (−19.7 ppm, $w_{1/2}$ = 4.4 Hz)[6c] and clearly show the η^5 coordination mode of the Cp* ligand. These findings are consistent with those for known beryllium metallocene complexes, whereas the low-field shift relative to the homoleptic organoberyllium compounds can be explained by the electron-withdrawing influence of the halide substituent.

Attempted Synthesis of Cp*BeF (4) and Unexpected Formation of $Cp^*{}_2Be$ (5). Several procedures were applied to synthesize Cp*BeF (**4**). Heteroleptic cyclopentadienyl beryllium complexes CpBeX have been prepared by the reaction between beryllocene and the corresponding disubstituted beryllium compound BeX_2.[3] Since the previous attempts by Drew and Morgan[21] to synthesize CpBeF by the reaction of Cp_2Be and BeF_2 failed, we did not investigate the analogous reaction with $Cp^*{}_2Be$. Moreover, salt elimination reactions were expected to be rather problematic because of the insolubility of BeF_2 in organic solvents. We therefore investigated the reactions of **1**−**3** with well-established fluorinating reagents, including oxidizing reagents such as AgF_2, XeF_2, and $4\text{-}FC_6H_4IF_2$ as well as "salt elimination" reagents such as AgF, NaF, and Me_4NF (Scheme 2).

Scheme 2. Attempted Synthesis of Cp*BeF (4) and Synthesis of $Cp^*{}_2Be$ (5)

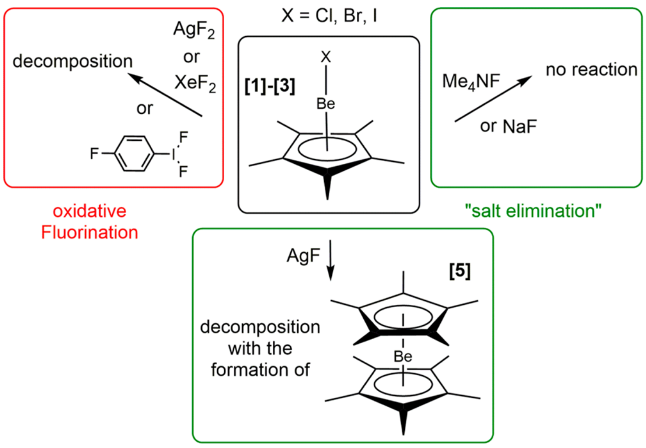

Unfortunately, mixing of **1**, **2**, or **3** with one of the oxidizing reagents as solid powders in the glovebox led to tremendous flames, even though they were under an argon atmosphere, which impressively demonstrated the reactivity of these compounds; the reactions yielded black amorphous powders and several nonidentifiable organic decomposition products. Analogous reactions at low temperature (−78 °C) in highly diluted solutions in toluene also did not yield **4**. In contrast, reactions of suspensions of NaF or Me_4NF in toluene with **1**−**3** did not lead to any products, as was proven with ^{9}Be NMR spectroscopy, and even after several days only the starting materials could be isolated. In contrast, a suspension of AgF and **3** in toluene immediately turned dark and yielded a black insoluble powder and a yellow solution. The black solid was a mixture of elemental silver and silver iodide, whereas the yellow solution contained $Cp^*{}_2Be$ (**5**), which crystallized upon concentration and cooling of the toluene solution. The NMR data and the unit cell of the measured crystal were consistent with the previously described structure. We first suggested that this reaction occurred as a result of a light-induced redox reaction of AgI, which is formed during the salt elimination

Table 1. ^{9}Be NMR Shifts [ppm] of Homo- and Heteroleptic CpBe and Cp*Be Compounds in Various Solvents

solvent	Cp*BeCl[a]	Cp*BeBr[a]	Cp*BeI[a]	$Cp^*{}_2Be$[6c]	Cp*BeCp′[6c]	Cp_2Be[9b]
C_6D_6	−14.88	−14.81	−15.78	−21.7	−19.7	–
toluene-d_8	−14.94	−14.85	−15.77	–	–	–
THF-d_8	−15.20	−15.08	−16.00	–	–	–
Cy-d_{12}[b]	–	–	–	–	–	−21.9
^{Me}Cy[c]	–	–	–	–	–	−18.3

[a]This work. [b]Cy = cyclohexane. [c]^{Me}Cy = methylcyclohexane.

reaction, but the strict avoidance of light (brown glassware and dark fume hood) gave the same results.

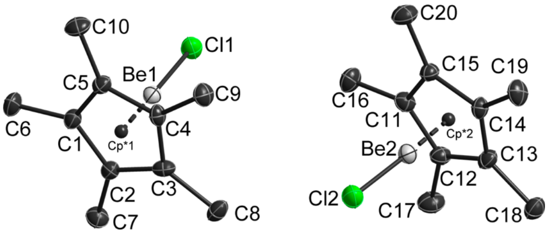

Figure 1. Solid-state structure of **1**. Thermal ellipsoids are shown at the 50% probability level, and hydrogen atoms have been omitted for clarity.

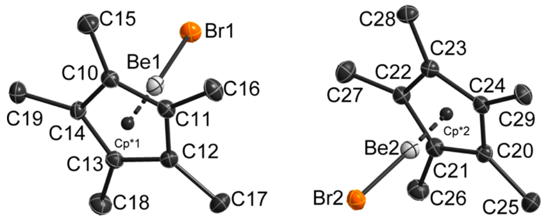

Figure 2. Solid-state structure of **2**. Thermal ellipsoids are shown at the 50% probability level, and hydrogen atoms have been omitted for clarity.

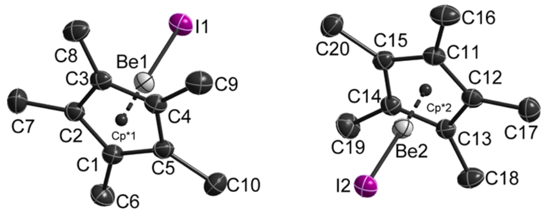

Figure 3. Solid-state structure of **3**. Thermal ellipsoids are shown at the 50% probability level, and hydrogen atoms have been omitted for clarity.

Solid-State Structures. Single crystals of **1**–**3** were grown from solutions in toluene at −28 °C, and Figures 1–3 show the crystal structures. **1**–**3** crystallize with two independent molecules in the monoclinic space group $P2_1/c$ (**1** and **3**) or $P\bar{1}$ (**2**) as colorless crystals. Table S1 in the Supporting Information summarizes the crystallographic details, and Table 2 gives the most important structural parameters of **1**–**3** and of other structurally characterized Cp*Be complexes. The Cp* ligands are η^5-bonded to the Be atoms, and the Cp* centroid (Cp*$_{\text{centr}}$)−Be bond lengths in **1**–**3** become marginally shorter with increasing atomic number of the halide substituent (1.4401 and 1.4393 Å in **1**, 1.4241 and 1.4348 Å in **2**, and 1.4165 and 1.4254 Å in **3**), while the Be−X bond lengths increase with increasing atomic number of the halide (1.879(4) and 1.879(4) Å in **1**, 2.031(3) and 2.032(3) Å in **2**, and 2.251(4) and 2.238(4) Å in **3**). The Cp*$_{\text{centr}}$−Be−X bond angles in **1**–**3** are close to 180°. Because of the lack of heteroleptic cyclopentadienyl beryllium halides, the Be−Cl bond lengths of **1** can only be compared with the one reported for CpBeCl (1.869(3) Å),[12a] which is almost identical. The Cp$_{\text{centr}}$−Be bond length in η^5-CpBeCl (1.451(5) Å) is somewhat longer than the Cp*$_{\text{centr}}$−Be bond length in **1** despite the smaller steric demand of the Cp ligand (Table 1). The Cp*$_{\text{centr}}$−Be bond length reported for Cp*$_2$Be (1.471(7) Å) is marginally elongated compared with those observed in **1**–**3**.[6a,c,d] In the packing, the molecules of **1**–**3** form centrosymmetric dimers connected by CH···π interactions (Figure 4 and Table 3).

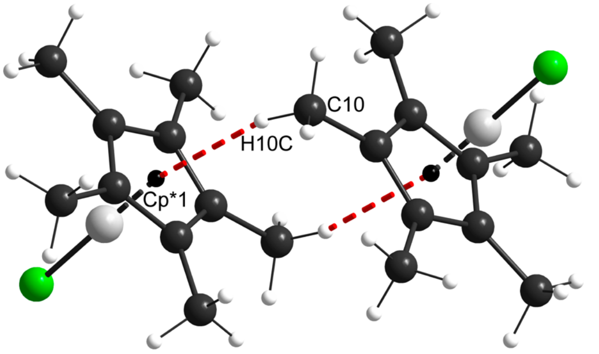

Figure 4. Centrosymmetric dimer formed by CH···π interactions (example taken from the structure of **1**).

1–**3** are Be analogues of classical Grignard compounds (RMgX), which are typically obtained as donor-stabilized dimeric molecules of the general type [Cp*MgX(Do)]$_2$ (Do = donor solvent), such as [Cp*MgBr(O=CHNMe$_2$)]$_2$,[22] [Cp*Mg(thf)(μ-Cl)]$_2$,[23] [Cp*Mg(OEt$_2$)(μ-Cl)]$_2$,[24] and [Mg$_2$Br$_2$Cp*$_2$(thf)].[25] Comparable findings were reported for

Table 2. Interatomic Distances and Angles in 1–3 and Related Cp*BeR Compounds

	Be−X [Å]	Cp*$_{\text{centr}}$−Be [Å]	Cp*$_{\text{centr}}$−Be−X [deg]	ref
1	1.879(4), 1.879(4)	1.4393, 1.4401	178.07, 178.85	this work
2	2.031(3), 2.032(3)	1.4241, 1.4348	177.49, 178.78	this work
3	2.251(4), 2.238(4)	1.4165, 1.4254	178.07, 179.14	this work
CpBeCl	1.869(3)	1.451(5)	178.4(3)	12a
Cp*Be−F−Al(OR^F)$_3$	1.502(7)	1.400	–	13
Cp*$_2$Be	–	1.655(1)	180	6a,c,d
Cp*BeCp′[a]	–	1.471(7)	–	6b,c
Cp*BeC(Cp′)=NR[b]	–	1.470(4)	178.2(2)	11
Cp*BeC(Cp*)=NR[b]		1.472(4)	178.7(5)	11, 18
Cp*BeP(*t*-Bu)$_2$	–	1.48(1)	168.3(7)	19
Cp*BeAs(*t*-Bu)$_2$	–	1.48(1)	171.9(5)	20
Cp*$_2$YbMeBeCp*	–	1.45	–	17

[a] Cp′ = C_5Me_4H. [b] R = 2,6-$Me_2C_6H_3$.

Table 3. Geometrical Data for the CH···π Interactions

compound	interaction[a]	symmetry operator	H···Cp^*_{centr} [Å]	C−H···Cp^*_{centr} [deg]
1	C19−H19A···Cp^*_{centr}2	$-x + 2, -y + 1, -z$	2.74	159.0
	C10−H10C···Cp^*_{centr}1	$-x + 1, -y + 1, -z + 1$	2.61	164.0
2	C16−H16A···Cp^*_{centr}2	$-x + 2, -y + 1, -z$	2.65	160.1
	C7−H7C···Cp^*_{centr}1	$-x + 1, -y, -z + 1$	2.75	163.5
3	C20−H20C···Cp^*_{centr}2	$-x + 1, -y, -z + 1$	2.68	159.6
	C8−H8C···Cp^*_{centr}1	$-x + 2, -y + 1, -z + 1$	2.86	154.2

[a] Cp^*_{centr} denotes the centroid of the Cp* ligand. See Figures 1−3.

the heavier Ca analogue $[Cp^*Ca(thf)_2(\mu\text{-}I)]_2$.[26] However, the Lewis acidity of homoleptic cyclopentadienyl beryllium complexes is rather less, and as a consequence, these complexes are typically obtained as solvent-free molecules. In addition, Schnöckel and co-workers reported the solid-state structures of several anionic Grignard derivatives such as $[Mg_3Cl_4Cp^*_3]^-$, $[Mg_6Br_8Cp^*_5]^-$, $[Mg_2I_3Cp^*_2]^-$,[27] and $[Mg_6Cl_8Cp^*_5]^-$,[28] which were claimed as final intermediates on the way to the molecular donor-free Grignard reagent Cp*MgX. Of particular interest are $[Mg_6Cl_8Cp^*_5]^-$ and $[Mg_6Br_8Cp^*_5]^-$, since these contain inverse-sandwich-like MgCp*Mg moieties.

Computational Studies. Gas-phase structures of **1**−**4** were calculated using the crystal structures as starting points for geometry optimizations with density functional theory (DFT) methods employing the B3LYP functional[29] and the def2-TZVPP basis set,[30] using relativistic effective core potentials (def2-ecp)[32] for I, and the resolution of the identity (RI) approximation[31] as implemented in the TURBOMOLE program package.[32]

The calculated structures **1′**−**4′** show Cp^*_{centr}−Be−X angles of approximately 180° and approximate C_{5v} symmetry with one hydrogen atom of each methyl group pointing away from the Be atom. While the Be−X distance increases in going from X = F to X = I, the Cp^*_{centr}−Be distance marginally decreases, which is in accordance with the trends observed in the crystal structures. The calculated distances are in good agreement with the average distances obtained from the crystal structures (Table 4).

Table 4. Comparison of Calculated and Experimental Be−X and Cp^*_{centr}−Be lengths [Å]

		X = F	X = Cl	X = Br	X = I
Be−X	calcd	1.42	1.88	2.04	2.26
	XRD	−	1.879(4), 1.879(4)	2.031(3), 2.032(3)	2.251(4), 2.238(4)
Cp^*_{centr}−Be	calcd	1.48	1.46	1.45	1.45
	XRD	−	1.4393, 1.4401	1.4241, 1.4348	1.4165, 1.4254

The slight deviation of the Cp^*_{centr}−Be−X angle in the crystal structures (~178−179°) from 180° seems to be due to crystal packing effects. The differences between the calculated Cp^*_{centr}−Be and Be−X distances and those observed in the crystal structures are less than 3%. The decrease in the Cp^*_{centr}−Be distance, while consistent between the calculations and the crystal structures, lies very close to the accuracy of the methods and will not be discussed any further. The increase in the Be−X distance, while dampened by increasing covalent character of the bond, is to be expected on the basis of the increasing van der Waals radius of the halide.

Natural bond orbital (NBO) analyses of **1′**−**4′** show decreasing absolute charges on the Be atom (1.72 in **4′** (F), 1.57 in **1′** (Cl), 1.51 in **2′** (Br), and 1.44 in **3′** (I)) as well as on the halide atom (F, −0.87; Cl, −0.74; Br, −0.69; I, −0.62) with increasing atomic number of the halide substituent X, while the average charge on the C atoms of the Cp* ring (C_{ring}) is approximately constant (−0.21). In addition, electron localization function (ELF)[33] and localized orbital locator (LOL)[34] calculations were performed on the resulting structures. Figure 5 shows 2D plots of the ELF along the C_{ring}−Be−X plane, and Figure 6 shows 3D renderings of the LOL (at ν = 0.525). The decreasing charges are evidence of the increasing covalent character of the Be−X bond, which is further supported by the ELF plots and LOL renderings.

The ELF plots clearly show that the bonding between Be and Cp* does not change with decreasing electronegativity of the halide substituent, while small changes between the halide and Be atoms are apparent (Figure 5). While still being predominantly ionic, which can be seen by the very low η values around Be, the beryllium−halide bond becomes more covalent, as reflected in a change in the shape of the ELF around the halide in the vicinity of Be. Also, the polarization of the Cp* ligand by Be is apparent from the asymmetric shape of the ELF around it concerning the ring plane. Naturally, the Cp*−Be interaction shows some covalent contributions.

The LOL renderings further demonstrate the increase in covalence of the beryllium−halide bond with increasing atomic number of the halide atom (Figure 6). As the rendered surfaces (ν = 0.525) contain regions where electrons are slower than they would be in the uniform electron gas (ν = 0.5), the covalent bonding contribution can be visualized. While the surfaces around F and Cl are still attached to those occurring at the atoms themselves, they can be clearly seen between beryllium and the halide for Br and I, which demonstrates the increasing covalent character in going from F to I in an intuitive way. As was observed in the ELF plots, the interactions between the Cp* ligand and the Be atom are similar for all of the halides. Nevertheless, no descriptive quantitative value for the amount of covalent contribution to the beryllium−halide bond can be derived from LOL visualizations.

■ CONCLUSIONS

Three Be-analogous Grignard compounds of the type Cp*BeX (X = Cl, Br, I) were structurally characterized. The half-sandwich beryllocenes show η^5-bonded Cp* groups and in the solid state form centrosymmetric dimers connected by CH···π interactions. The structural parameters of the geometry-optimized structures of **1**−**3** agree very well with the experimental data. Natural bond orbital (NBO) analyses show decreasing absolute charges of the Be atom and the halide atom with increasing atomic number of the halide substituent, as was expected, while the average charge on the C

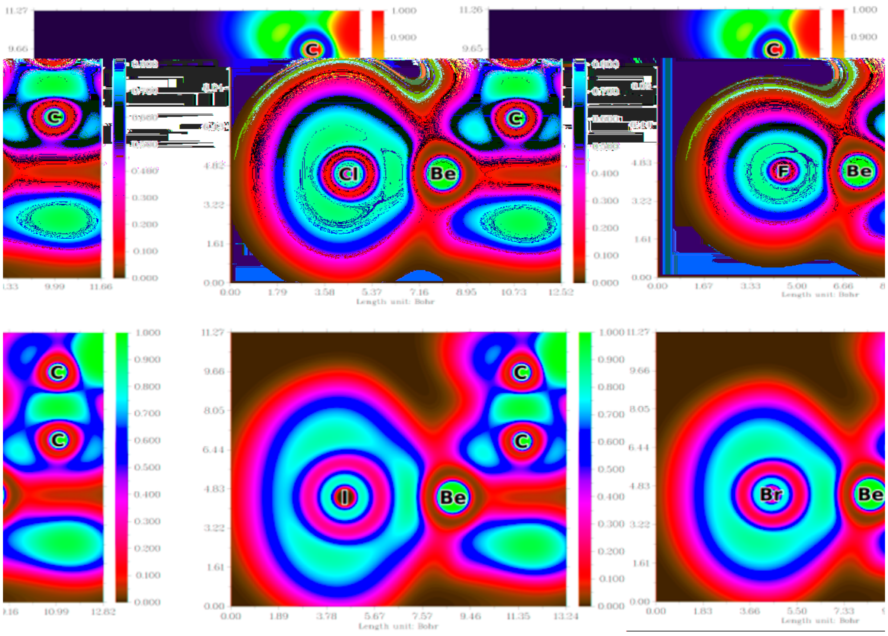

Figure 5. 2D ELF plots for **1**−**4** in the C_{ring}−Be−X plane.

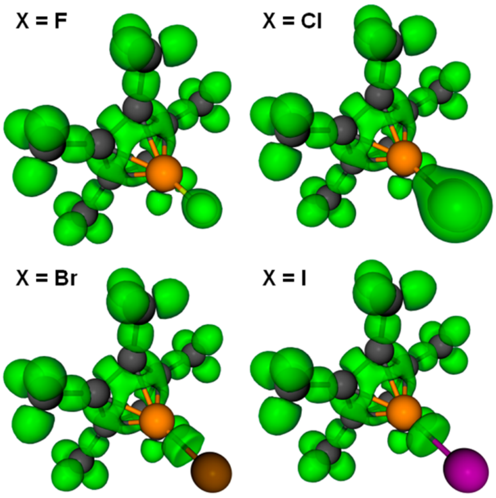

Figure 6. 3D LOL plots of **1**−**4** with ν = 0.525.

atoms of the Cp* ring is approximately constant. Electron localization function (ELF) and localized orbital locator (LOL) calculations show an increasing covalent character of the Be−X bond with increasing atomic number of the halide substituent.

■ EXPERIMENTAL DETAILS

CAUTION! Beryllium and its compounds are regarded as highly toxic[35] and carcinogenic and have an allergenic potential if inhaled with the risk of causing chronic beryllium disease (CBD). They should therefore be handled with appropriate safety precautions, and all experiments described herein were performed in fume hoods, in gloveboxes, or with standard Schlenk techniques under an Ar atmosphere. Dry solvents were obtained from a solvent purification system (MBraun) and degassed prior to use. NMR spectra were recorded on a Bruker Avance 300 spectrometer at 25 °C at 300.1 MHz (^{1}H), 42.2 MHz (^{9}Be), or 75.5 MHz (^{13}C) and referenced to internal C_6D_5H ($\delta(^{1}H)$ = 7.154 ppm; $\delta(^{13}C)$ = 128.0 ppm), internal THF-d_8 ($\delta(^{1}H)$ = 3.58, 1.72 ppm; $\delta(^{13}C)$ = 25.31, 67.21 ppm), internal toluene-d_8 ($\delta(^{1}H)$ = 2.08, 6.97, 7.01, 7.09 ppm; $\delta(^{13}C)$ = 20.43, 125.13, 127.96, 128.87, 137.48 ppm) or external $BeSO_4$ in D_2O ($\delta(^{9}Be)$ = 0 ppm).[36] Elemental analyses were not determined because of the potential toxicity of the complexes. The purity of the compounds was verified by NMR spectroscopy. BeX_2 (X = Cl, Br, I) was synthesized from the elements at elevated temperatures followed by high-temperature, high-vacuum fractional sublimation.[37]

General Procedure for the Synthesis of Cp*BeX (X = Cl (1), Br (2), I (3)). Equimolar amounts of Cp*K (2.500 g, 14 mmol) and BeX_2 (X = Cl, 1.146 g, 14 mmol; X = Br, 2.363 g, 14 mmol; X = I, 3.679 g, 14 mmol) were mixed in toluene (50 mL) at ambient temperature, and the mixture was stirred for 16 h. After filtration of the insoluble precipitate, the solvent was reduced in vacuo to 3 mL. **1**−**3** were obtained in high yields as colorless crystalline solids after storage at −30 °C for 4 h. The analytical data for **1** and **2** agree with those reported in the literature.[11]

*Cp*BeCl (**1**).* Yield 2.163 g (86%). ^{1}H NMR (300 MHz, C_6D_6, 25 °C): δ = 1.68 (s, 15H, $BeC_5(CH_3)_5Cl$) ppm. ^{9}Be (42.2 MHz, C_6D_6): δ = −14.88 (s, $BeC_5(CH_3)_5Cl$) ppm. ^{13}C NMR (125 MHz, C_6D_6, 25 °C): δ = 9.05 ($BeC_5(CH_3)_5Cl$), 109.95 ($BeC_5(CH_3)_5Cl$) ppm. ^{1}H NMR (300 MHz, toluene-d_8, 25 °C): δ = 1.70 (s, 15H, $BeC_5(CH_3)_5Cl$) ppm. ^{9}Be (42.2 MHz, toluene-d_8): δ = −14.94 (s, $BeC_5(CH_3)_5Cl$) ppm. ^{13}C NMR (125 MHz, toluene-d_8, 25 °C): δ = 8.61 ($BeC_5(CH_3)_5Cl$), 109.55 ($BeC_5(CH_3)_5Cl$) ppm. ^{1}H NMR (300 MHz, THF-d_8, 25 °C): δ = 1.96 (s, 15H, $BeC_5(CH_3)_5Cl$) ppm. ^{9}Be (42.2 MHz, THF-d_8): δ = −15.20 (s, $BeC_5(CH_3)_5Cl$) ppm. ^{13}C NMR (125 MHz, THF-d_8, 25 °C): δ = 9.00 ($BeC_5(CH_3)_5Cl$), 110.41 ($BeC_5(CH_3)_5Cl$) ppm.

*Cp*BeBr (**2**).* Yield 2.667 g (85%). ^{1}H NMR (300 MHz, C_6D_6, 25 °C): δ = 1.67 (s, 15H, $BeC_5(CH_3)_5Br$) ppm. ^{9}Be (42.2 MHz, C_6D_6): δ = −14.81 (s, $BeC_5(CH_3)_5Br$) ppm. ^{13}C NMR (125 MHz, C_6D_6, 25 °C): δ = 9.10 ($BeC_5(CH_3)_5Br$), 110.21 ($BeC_5(CH_3)_5Br$) ppm. ^{1}H NMR (300 MHz, toluene-d_8, 25 °C): δ = 1.69 (s, 15H, $BeC_5(CH_3)_5Br$) ppm. ^{9}Be (42.2 MHz, toluene-d_8): δ = −14.85 (s, $BeC_5(CH_3)_5Br$) ppm. ^{13}C NMR (125 MHz, toluene-d_8, 25 °C): δ = 8.30 ($BeC_5(CH_3)_5Br$), 109.57 ($BeC_5(CH_3)_5Br$) ppm. ^{1}H NMR (300 MHz, THF-d_8, 25 °C): δ = 1.96 (s, 15H, $BeC_5(CH_3)_5Br$) ppm. ^{9}Be (42.2 MHz, THF-d_8): δ = −15.08 (s, $BeC_5(CH_3)_5Br$) ppm. ^{13}C NMR (125 MHz, THF-d_8, 25 °C): δ = 9.08 ($BeC_5(CH_3)_5Br$), 110.68 ($BeC_5(CH_3)_5Br$) ppm.

*Cp*BeI (**3**).* Yield 3.492 g (92%). ^{1}H NMR (300 MHz, C_6D_6, 25 °C): δ = 1.65 (s, 15H, $BeC_5(CH_3)_5I$) ppm. ^{9}Be (42.2 MHz, C_6D_6): δ = −15.78 (s, $BeC_5(CH_3)_5I$) ppm. ^{13}C NMR (125 MHz, C_6D_6, 25 °C): δ = 9.27 ($BeC_5(CH_3)_5I$), 110.53 ($BeC_5(CH_3)_5I$) ppm. ^{1}H NMR (300 MHz, toluene-d_8, 25 °C): δ = 1.67 (s, 15H, $BeC_5(CH_3)_5I$) ppm. ^{9}Be (42.2 MHz, toluene-d_8): δ = −15.77 (s, $BeC_5(CH_3)_5I$) ppm. ^{13}C NMR

DOI: 10.1021/acs.organomet.5b00389
Organometallics XXXX, XXX, XXX−XXX

(125 MHz, toluene-d_8, 25 °C): δ = 8.84 ($BeC_5(CH_3)_5I$), 110.13 ($BeC_5(CH_3)_5I$) ppm. ^1H NMR (300 MHz, THF-d_8, 25 °C): δ = 1.97 (s, 15H, $BeC_5(CH_3)_5I$) ppm. ^9Be (42.2 MHz, THF-d_8): δ = −16.00 (s, $BeC_5(CH_3)_5I$) ppm. ^{13}C NMR (125 MHz, THF-d_8, 25 °C): δ = 9.29 ($BeC_5(CH_3)_5I$), 111.00 ($BeC_5(CH_3)_5I$) ppm.

Single-Crystal X-ray Analyses. Crystallographic data for **1**−**3**, which were collected on a Bruker AXS APEX 2 diffractometer (Mo Kα radiation, λ = 0.71073 Å), are summarized in Table S1 in the Supporting Information. Figures 1−3 show diagrams of the solid-state structures of **1**−**3**. Data were collected at 121(1) K (**1**), 100(1) K (**2**), and 150(1) K (**3**). The structures were solved by direct methods (SHELXS-97) and refined anisotropically by full-matrix least-squares on F^2 (SHELXL-97/SHELXL2013).[38] Absorption corrections were performed semiempirically from equivalent reflections on the basis of multiscans (Bruker AXS APEX2). **1** was a nonmerohedral twin of two components of approximately equal size and refined against HKL5 data. Absorption correction was performed with TWINABS.

The crystallographic data for **1**−**3** (excluding structure factors) have been deposited with the Cambridge Crystallographic Data Centre (CCDC) as supplementary publications CCDC-1051315 (**1**), CCDC-1051317 (**2**), and CCDC-1051316 (**3**). Copies of the data can be obtained free of charge upon application to the CCDC, 12 Union Road, Cambridge CB2 1EZ, U.K. (fax: (+44) 1223/336033; e-mail: deposit@ccdc.cam-ak.uk).

■ ASSOCIATED CONTENT

Ⓢ Supporting Information

A CIF file giving X-ray crystallographic data for **1**−**3**; crystallographic details for **1**−**3** and **5**; ^1H, ^9Be, and ^{13}C NMR data for **1**−**3**; and computational details (gas-phase structures, NBO analyses, and ELF and LOL plots) for **1**−**3**. The Supporting Information is available free of charge on the ACS Publications website at DOI: 10.1021/acs.organomet.5b00389.

■ AUTHOR INFORMATION

Corresponding Author

*Phone: +49 0201-1834635. Fax: + 49 0201-1833830. E-mail: stephan.schulz@uni-due.de.

Author Contributions

The manuscript was written through contributions of all authors. All authors have given approval to the final version of the manuscript.

Notes

The authors declare no competing financial interest.

■ ACKNOWLEDGMENTS

S.S. thanks the University of Duisburg-Essen for financial support. We thank Materion Company for the donation of beryllium metal.

■ REFERENCES

(1) (a) Hanusa, T. P. *Organometallics* **2002**, *21*, 2559−2571. (b) Jutzi, P.; Burford, N. *Chem. Rev.* **1999**, *99*, 969−990. (c) Jutzi, P.; Burford, N. In *Metallocenes: Synthesis, Reactivity, Applications*; Togni, A., Halterman, R. L., Eds.; Wiley-VCH: Weinheim, Germany, 1998; Vol. *1*, Chapter 1. (d) Bell, N. A. In *Comprehensive Organometallic Chemistry II*; Wilkinson, G., Stone, F. G. A., Abel, E. W., Eds.; Pergamon Press: Oxford, U.K., 1995; Vol. *1*, Chapter 2. (e) Hays, M. L.; Hanusa, T. P. *Adv. Organomet. Chem.* **1996**, *40*, 117−170. (f) Stalke, D. *Angew. Chem.* **1994**, *106*, 2256−2259; *Angew. Chem., Int. Ed. Engl.* **1994**, *33*, 2168−2171. (g) Budzelaar, P. H. M.; Engelberts, J. J.; van Lenthe, J. H. *Organometallics* **2003**, *22*, 1562−1576.

(2) (a) Rayon, V. M.; Frenking, G. *Chem.—Eur. J.* **2002**, *8*, 4693−4707. (b) Kwon, O.; McKee, M. L. In *Computational Organometallic Chemistry*; Cundan, T. R., Ed.; Marcel Dekker: New York, 2001; p 397.

(3) Fernández, R.; Carmona, E. *Eur. J. Inorg. Chem.* **2005**, 3197−3206.

(4) (a) Fischer, E. O.; Hofmann, H. P. *Chem. Ber.* **1959**, *92*, 482−486. (b) Fischer, E. O.; Schreiner, S. *Chem. Ber.* **1959**, *92*, 938−948. (c) Strohmeier, W.; von Hobe, D. *Z. Elektrochem.* **1960**, *64*, 945−951. (d) Pratten, S. J.; Cooper, M. K.; Aroney, M. J.; Filipczuk, S. W. *Dalton Trans.* **1985**, 1761−1765.

(5) (a) Nugent, K. W.; Beattie, J. K.; Hambley, T. W.; Snow, M. R. *Aust. J. Chem.* **1984**, *37*, 1601−1606. (b) Wong, C. H.; Lee, T. Y.; Chao, K. J.; Lee, S. *Acta Crystallogr., Sect. B* **1972**, *28*, 1662−1665. (c) Wong, C. H.; Lee, T. Y.; Lee, T. J.; Chang, T. W.; Liu, C. S. *Inorg. Nucl. Chem. Lett.* **1973**, *9*, 667−673.

(6) (a) del Mar Conejo, M.; Fernández, R.; Gutiérrez-Puebla, E.; Monge, Á.; Carmona, E. *Angew. Chem.* **2000**, *112*, 2025−2027; *Angew. Chem., Int. Ed.* **2000**, *39*, 1949−1951. (b) del Mar Conejo, M.; Fernández, R.; del Río, D.; Carmona, E.; Monge, Á.; Ruiz, C. *Chem. Commun.* **2002**, 2916−2917. (c) del Mar Conejo, M.; Fernández, R.; del Río, D.; Carmona, E.; Monge, Á.; Ruiz, C.; Márquez, A. M.; Sanz, J. F. *Chem.—Eur. J.* **2003**, *9*, 4452−4461. (d) Hung, I.; Macdonald, C. L. B.; Schurko, R. W. *Chem.—Eur. J.* **2004**, *10*, 5923−5935.

(7) Almenningen, A.; Haaland, A.; Lusztyk, J. *J. Organomet. Chem.* **1979**, *170*, 271−284.

(8) (a) Marinyk, D. S. *J. Am. Chem. Soc.* **1977**, *99*, 1436−1441. (b) Chiu, N. S.; Schäfer, L. *J. Am. Chem. Soc.* **1978**, *100*, 2604−2607. (c) Jemmis, E. D.; Alexandratos, S.; Schleyer, P. v. R.; Streitwieser, A., Jr.; Schaefer, H. F., III. *J. Am. Chem. Soc.* **1978**, *100*, 5695−5700. (d) Gleiter, R.; Böhm, M.; Haaland, A.; Johansen, R.; Lusztyk, J. *J. Organomet. Chem.* **1979**, *170*, 285−292.

(9) (a) Wong, C.; Wang, S. *Inorg. Nucl. Chem. Lett.* **1975**, *11*, 677−678. (b) Nugent, K. W.; Beattie, J. K.; Field, L. D. *J. Phys. Chem.* **1989**, *93*, 5371−5377.

(10) (a) Margl, P.; Schwarz, K.; Blöchl, P. E. *J. Chem. Phys.* **1995**, *103*, 683−690. (b) McKee, M. L. *Wiley Interdiscip. Rev.: Comput. Mol. Sci.* **2011**, *1*, 943−951.

(11) del Mar Conejo, M.; Fernández, R.; Carmona, E.; Andersen, R. A.; Gutiérrez-Puebla, E.; Monge, M. A. *Chem.—Eur. J.* **2003**, *9*, 4462−4471.

(12) (a) Goddard, R.; Akhtar, J.; Starowieyski, K. B. *J. Organomet. Chem.* **1985**, *282*, 149−154. (b) Saulys, D. A.; Powell, D. R. *Organometallics* **2003**, *22*, 407−413.

(13) Himmel, D.; Scheer, H.; Kratzert, D.; Krossing, I. *Z. Anorg. Allg. Chem.* **2015**, *641*, 655−659.

(14) (a) Naglav, D.; Bläser, D.; Wölper, C.; Schulz, S. *Inorg. Chem.* **2014**, *53*, 1241−1249. (b) Naglav, D.; Neumann, A.; Bläser, D.; Wölper, C.; Haack, R.; Jansen, G.; Schulz, S. *Chem. Commun.* **2015**, *51*, 3889−3891.

(15) Burns, C. J.; Andersen, R. A. *J. Organomet. Chem.* **1987**, *325*, 31−37.

(16) Pratten, S. J.; Cooper, M. K.; Aroney, M. J. *J. Organomet. Chem.* **1990**, *381*, 147−153.

(17) Burns, C. J.; Andersen, R. A. *J. Am. Chem. Soc.* **1987**, *109*, 5853−5855.

(18) del Mar Conejo, M.; Fernández, R.; Carmona, E.; Gutierrez-Puebla, E.; Monge, M. A. *Organometallics* **2001**, *20*, 2434−2436.

(19) Atwood, J. L.; Bott, S. G.; Jones, R. A.; Koschmieder, S. U. *Chem. Commun.* **1990**, 692−693.

(20) Battle, S. L.; Cowley, A. H.; Decken, A.; Jones, R. A.; Koschmieder, S. U. *J. Organomet. Chem.* **1999**, *582*, 66−69.

(21) Drew, D. A.; Morgan, G. L. *Inorg. Chem.* **1977**, *16*, 1704−1708.

(22) Schnöckel, H.; Duan, T. Private Communication, 2005; CCDC 267694, DOI: 10.5517/cc8zk92.

(23) Cramer, R. E.; Richmann, P. N.; Gilje, J. W. *J. Organomet. Chem.* **1991**, *408*, 131−136.

(24) Dohmeier, C.; Loos, D.; Robl, C.; Schnöckel, H. *J. Organomet. Chem.* **1993**, *448*, 5−8.

(25) Vollet, J.; Hartig, J. R.; Schnöckel, H. *Angew. Chem.* **2004**, *116*, 3248−3252; *Angew. Chem., Int. Ed.* **2004**, *43*, 3186−3189.

(26) McCormick, M. J.; Craig-Sockwell, S.; Davies, C. E. H.; Hanusa, T. P.; Huffman, J. C. *Organometallics* **1989**, *8*, 2044−2049.

(27) Kruczyński, T.; Pushkarevsky, N.; Henke, P.; Köppe, R.; Baum, E.; Konchenko, S.; Pikies, J.; Schnöckel, H. *Angew. Chem.* **2012**, *124*, 9159−9163; *Angew. Chem., Int. Ed.* **2012**, *51*, 9025−9029.

(28) Vollet, J.; Hartig, J. R.; Baranowska, K.; Schnöckel, H. *Organometallics* **2006**, *25*, 2101−2103.

(29) (a) Becke, A. D. *J. Chem. Phys.* **1993**, *98*, 5648−5652. (b) Stephens, P. J.; Devlin, F. J.; Chabalowski, C. F.; Frisch, M. J. *J. Phys. Chem.* **1994**, *98*, 11623−11627.

(30) Weigend, F.; Ahlrichs, R. *Phys. Chem. Chem. Phys.* **1994**, *7*, 3297−3305.

(31) (a) Häser, M.; Ahlrichs, R. *J. Comput. Chem.* **1989**, *10*, 104−111. (b) Bauernschmitt, R.; Ahlrichs, R. *Chem. Phys. Lett.* **1996**, *256*, 454−464. (c) von Arnim, M.; Ahlrichs, R. *J. Comput. Chem.* **1998**, *19*, 1746−1757. (d) Sierka, M.; Hogekamp, A.; Ahlrichs, R. *J. Chem. Phys.* **2003**, *118*, 9136−9148. (e) Weigend, F. *Phys. Chem. Chem. Phys.* **2006**, *8*, 1057−1065.

(32) Ahlrichs, R.; Bär, M.; Häser, M.; Horn, H.; Kölmel, C. *Chem. Phys. Lett.* **1989**, *162*, 165−169.

(33) Becke, A. D.; Edgecombe, K. E. *J. Chem. Phys.* **1990**, *92*, 5397−5403.

(34) Schmider, H. L.; Becke, A. D. *J. Mol. Struct.: THEOCHEM* **2000**, *527*, 51−61.

(35) (a) Handa, T.; Nagai, S.; Kitaichi, M.; Chin, K.; Ito, Y.; Oga, T.; Takahashi, K.; Watanabe, K.; Mishima, M.; Izumi, T. *Sarcoidosis, Vasculitis Diffuse Lung Dis.* **2009**, *26*, 24−31. (b) Strupp, C. *Ann. Occup. Hyg.* **2011**, *55*, 43−56. (c) Strupp, C. *Ann. Occup. Hyg.* **2011**, *55*, 30−42. (d) Cummings, K. J.; Stefaniak, A. B.; Abbas Virji, M.; Kreiss, K. *Environ. Health Perspect.* **2009**, *117*, 1250−1256. (e) Bill, J. R.; Mack, D. G.; Falta, M. T.; Maier, L. A.; Sullivan, A. K.; Joslin, F. G.; Martin, A. K.; Freed, B. M.; Kotzin, B. L.; Fontenot, A. P. *J. Immunol.* **2005**, *175*, 7029−7037.

(36) Fulmer, G. R.; Miller, A. J. M.; Sherden, N. H.; Gottlieb, H. E.; Nudelman, A.; Stoltz, B. M.; Bercaw, J. E.; Goldberg, K. I. *Organometallics* **2010**, *29*, 2176−2179.

(37) Brauer, G. In *Handbook of Preparative Inorganic Chemistry*, 2nd ed.; Academic Press: New York, 1963; Vol. *1*, p 890.

(38) (a) Sheldrick, G. M. *Acta Crystallogr., Sect. A* **1990**, *46*, 467−473. (b) Sheldrick, G. M. *SHELXL-97: Program for the Refinement of Crystal Structures*; University of Göttingen: Göttingen, Germany, 1997. Also see: Sheldrick, G. M. *Acta Crystallogr., Sect. A* **2008**, *64*, 112−122.

DOI: 10.1021/acs.organomet.5b00389